

# Fluorescence-Based Siderophore Biosensor for the Determination of Bioavailable Iron in Oceanic Waters

Cathy K. S. Chung Chun Lam,<sup>†</sup> Timothy D. Jickells,<sup>‡</sup> David J. Richardson,<sup>§</sup> and David A. Russell<sup>\*,†</sup>

School of Chemical Sciences and Pharmacy, School of Environmental Sciences, and School of Biological Sciences, University of East Anglia, Norwich, NR4 7TJ, UK

With direct evidence that iron is the chemical limitation of phytoplankton growth, particularly in the Southern Ocean, it is increasingly important to develop new tools that provide direct measurement of the bioavailable iron fraction in oceanic waters. Here we report the development of a fluorescence quenching-based siderophore biosensor capable of the *in situ* measurement of this ultratrace Fe(III) fraction at ambient pH (~8). Parabactin was extracted from cultures of *Paracoccus denitrificans*. The purified siderophore was encapsulated within a spin-coated sol–gel thin film, which was subsequently incorporated in a flow cell system. The parabactin biosensor has been fully characterized for the detection of Fe(III) in seawater samples. The biosensor can be regenerated by lowering the pH of the flowing solution, thereby releasing the chelated Fe(III), enabling multiple use. The LOD of the biosensor was determined to be 40 pM, while for an Fe(III) concentration of 1 nM, a reproducibility with a RSD of 6% ( $n = 10$ ) was obtained. The accuracy of the biosensing system has been determined through analysis of a certified seawater reference sample. Samples from the Atlantic Ocean have been analyzed using the parabactin biosensor providing a concentration vs depth profile for the bioavailable Fe(III) fraction in the 50 pM–1 nM range.

The primary production of organic carbon by phytoplankton in the oceans is central to the maintenance of the oceanic food chain, to the cycling of contaminants, and to the air–sea exchange of CO<sub>2</sub> and hence climate regulation.<sup>1</sup> Until recently, it had been assumed that marine primary production was limited by the supply of light or macronutrients such as nitrogen (mainly as nitrate) and dissolved inorganic phosphorus.<sup>2</sup> It has become evident over the last 10 years that other factors play a role, particularly in the Southern Ocean. In these areas, it has been proposed that the supply of iron is the chemical limitation of phytoplankton growth and there is now direct evidence for such iron limitation,

particularly from the ocean “iron seeding” experiments conducted at a variety of locations.<sup>3–5</sup> Iron is delivered to the oceans mainly in the form of soil dust with limited solubility, and it is regions furthest from sources of soil dust,<sup>4,6</sup> such as the Southern Ocean, where primary production appears to be limited by iron availability. It has been suggested that increases in iron supply during the last glaciation may have subsequently increased primary production, maintaining or possibly even creating the glacial climate.<sup>7,8</sup>

Recognition of the role of iron poses major challenges for environmental life scientists. It is important to understand the factors regulating iron concentrations in the oceans and, in turn, how phytoplankton react to, and themselves regulate, the concentration of iron. To achieve such an understanding, the ability to measure iron rapidly at the extremely low concentrations observed in oceanic waters (~50 pM) is required. Previously, samples have been collected and returned to the laboratory for analysis using graphite furnace atomic absorption spectroscopy.<sup>9</sup> However, such techniques are slow, cannot provide results at sea to inform shipboard operational planning, and cannot be adapted for remote operation. More recently, electrochemical<sup>10,11</sup> and flow injection spectrophotometric/chemiluminescence<sup>12,13</sup> techniques have been developed. The latter technique requires preconcentration of the iron species, and additionally, the chemiluminescence detection approach, while sensitive, requires a further reduction step prior to analysis as it is only measures Fe(II). Measurement of the Fe(II) fraction, with subsequent reduction of the sample to give a total iron concentration value, is a significant limitation as the vast majority (99.9%) of the dissolved iron in the oceans is reported to be in the form of organic complexes of Fe(III).<sup>14</sup> The key issue

(3) Boyd, P. W. *Deep-Sea Res., Part II* **2002**, *49*, 1803–1821.

(4) Turner, D. R.; Hunter, K. A. *The Biogeochemistry of Iron in Seawater*; John Wiley & Sons, Ltd.: Chichester, 2001.

(5) Song, J. *Acta Oceanol. Sin.* **2003**, *22*, 57–68.

(6) Jickells T. D.; An, Z. S.; Andersen, K. K.; Baker, A. R.; Bergametti, G.; Brooks, N.; Cao, J. J.; Boyd, P. W.; Duce, R. A.; Hunter, K. A.; Kawahata, H.; Kubilay, N.; laRoche, J.; Liss, P. S.; Mahowald, N.; Prospero, J. M.; Ridgwell, A. J.; Tegen, I.; Torres, R. *Science* **2005**, *208*, 65–71.

(7) Martin, J. H. *Palaeoceanography* **1990**, *5*, 1–13.

(8) Falkowski, P. G.; Barber, R. T.; Smetacek, V. *Science* **1998**, *281*, 200–206.

(9) Gordon, R. M.; Martin, J. H.; Knauer, G. A. *Nature* **1982**, *299*, 611–612.

(10) van den Berg, C. M. G.; Nimmo, M.; Abollino, O.; Mentasti, E. *Electroanalysis* **1991**, *3*, 477–484.

(11) Rue, E. L.; Bruland, K. W. *Limnol. Oceanogr.* **1997**, *42*, 901–910.

(12) Measures, C. I.; Yuan, J.; Resing, J. A. *Mar. Chem.* **1995**, *50*, 3–12.

(13) Bowie, A. R.; Achterberg, E. P.; Mantoura, R. F. C.; Worsfold, P. J. *Anal. Chim. Acta* **1998**, *361*, 189–200.

\* To whom correspondence should be addressed. E-mail: d.russell@uea.ac.uk.

<sup>†</sup> School of Chemical Sciences and Pharmacy.

<sup>‡</sup> School of Environmental Sciences.

<sup>§</sup> School of Biological Sciences.

(1) Watson, A. J.; Bakker, D. C. E.; Ridgwell, A. J.; Boyd, P. W.; Law, C. S. *Nature* **2000**, *407*, 730–733.

(2) Morel, F. M. M.; Rueter, J. G.; Price, N. M. *Oceanography* **1991**, *4*, 56–61.

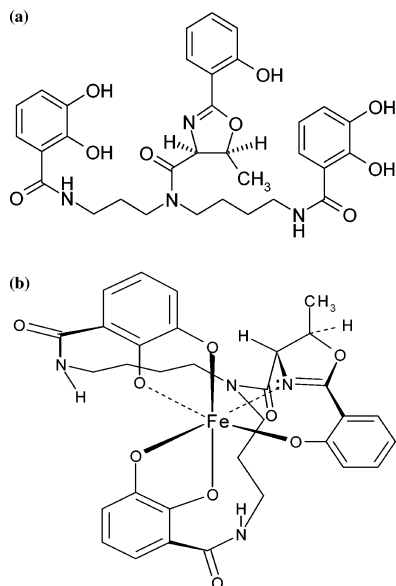


**Figure 1.** Structures of (a) parabactin and (b) the cyclic ferric parabactin complex.

for environmental scientists is the amount of iron in seawater that is “bioavailable” for uptake and subsequent utilization within cellular processes.

Iron in both soil and the oceans is often bound within complex organic and inorganic structures. To “extract” and use the iron for growth, microorganisms excrete iron chelators termed siderophores. There are a number of natural siderophores that are typically characterized by a high formation constant for Fe(III). To develop a device for the determination of the bioavailable iron fraction in oceanic waters, a siderophore with an exceptional Fe(III) binding constant would be an ideal choice for the molecular recognition element of the sensor. Such a siderophore would provide the potential for good sensitivity and selectivity and, importantly, provide a detection system that would mimic the biological uptake process. Measurements with this sensor would provide direct data of the bioavailable iron fraction. Parabactin (Figure 1a), first identified by Tait,<sup>15,16</sup> is a linear spermidine-containing catechol-type siderophore. Parabactin is soluble in solvents such as ethanol, methanol, ethyl acetate, and ether but only slightly soluble in water except at pH values above 8.0.<sup>16</sup> When Fe(III) is added to parabactin at neutral pH, a wine-red complex is obtained, with a formation constant,  $K_f$ , of  $\sim 10^{48} \text{ M}^{-1}$ .<sup>17,18</sup> Parabactin forms a hexadentate complex with iron(III). The iron induces a significant conformational change of the siderophore by coordinating to the four oxygens of the two catechol groups while the fifth and sixth ligands are associated with the 2-(2-hydroxy)oxazoline group (Figure 1b). Parabactin is a catecholamide, and its structure suggests that the molecule should exhibit fluorescence emission, although this has not been previously reported. As iron is an inherent excited-state quencher,

the optical response of parabactin to Fe(III) complexation will be a significant quenching of the fluorescence intensity, quantifiable by the Stern–Volmer relationship, offering the basis for developing an analytical device. Once Fe(III) has bound to parabactin, the ferric parabactin complex can be dissociated by the addition of acid, which would enable a parabactin-based biosensor to be regenerated for further measurements. It should be noted that parabactin is itself stable at low pH.

To develop a biosensor based on parabactin, it is essential to incorporate the siderophore in a matrix that accommodates the conformational change necessary for Fe(III) complexation. A second important characteristic of the matrix is that it is optically transparent to allow the changing fluorescent signal to be measured. We, and others, have used sol–gel technology as a means of encapsulating biological molecules, especially proteins and enzymes, due to the nondenaturing processing conditions; see for example refs 19–22. Previously, a bulk sol–gel was used to entrap pyoverdine for the determination of Fe(III) in tap water.<sup>23</sup> The applicability of the sol–gel process to the development of biosensing devices is apparent as the sol–gel matrix is chemically inert and thermally stable,<sup>24</sup> and dependent on the chemical composition can be optically transparent down to 250 nm. Sol–gels can be fabricated in a variety of configurations, with thin films considered the most useful for sensors because of the short diffusion pathway for the analyte to interact with the biological recognition molecule. A key consideration for this present study is that, by encapsulating the parabactin in a sol–gel network, the siderophore would be in a liquid microenvironment and hence free to move and rotate, allowing for the molecular reorganization into a cyclic structure that accompanies binding with Fe(III).

In this paper, we report the development of a biosensor for the bioavailable Fe(III) component of iron species in oceanic waters. The biosensor is based on the bacterial siderophore, parabactin, which has been extracted from *Paracoccus denitrificans*. The parabactin was purified and subsequently encapsulated within a silica sol–gel thin film spin-coated onto a quartz substrate to produce the biosensor. The transduction principle of the parabactin biosensor is that of fluorescence quenching upon formation of the cyclic complex with Fe(III). The porous structure of the sol–gel thin film not only allowed the oceanic water to diffuse through the sensor matrix, enabling the Fe(III) ion to coordinate with the encapsulated parabactin, but additionally accommodated the conformational change of the siderophore necessary for Fe(III) chelation. The successful development of a biosensor system capable of the measurement of Fe(III) in oceanic water samples at the ultratrace level of  $\sim 50 \text{ pM}$ , with a high degree of selectivity for the target cation, is reported. Further, the biosensor was used to obtain an Fe(III) concentration–depth

- (14) Hutchins, D. A.; Witter, A. E.; Butler, A.; Luther, G. W. *Nature* **1999**, *400*, 858–861.  
 (15) Tait, G. H. *Biochem. Soc. Trans.* **1974**, *2*, 657–658.  
 (16) Tait, G. H. *Biochem. J.* **1975**, *146*, 191–204.  
 (17) Bergeron, R. J.; Dionis, J. B.; Elliott, G. T.; Kline, S. J. *J. Biol. Chem.* **1985**, *260*, 7936–7944.  
 (18) Bergeron, R. J.; Dionis, J. B.; Ingho, M. J. *J. Org. Chem.* **1987**, *52*, 144–149.

- (19) Ellerby, L. M.; Nishida, C. R.; Nishida, F.; Yamanaka, S. A.; Dunn, B.; Valentine, J. S.; Zink, J. I. *Science* **1992**, *255*, 1113–1115.  
 (20) Avnir, D.; Braun, S.; Lev, O.; Ottolenghi, M. *Chem. Mater.* **1994**, *6*, 1605–1614.  
 (21) Narang, U.; Prasad, P. N.; Bright, F. V.; Ramanathan, K.; Kumar, N. D.; Malhotra, B. D.; Kamalasanan, M. N.; Chandra, S. *Anal. Chem.* **1994**, *66*, 3139–3144.  
 (22) Blyth, D. J.; Aylott, J. W.; Richardson, D. J.; Russell, D. A. *Analyst* **1995**, *120*, 2725–2730.  
 (23) Barrero, J. M.; Camara, C.; Perezconde, M. C.; Sanjose, C.; Fernandez, L. *Analyst* **1995**, *120*, 431–435.  
 (24) Tang, Y.; Tehan, E. C.; Tao, Z.; Bright, F. V. *Anal. Chem.* **2003**, *75*, 2407–2413.

profile from seawater samples taken from the North Atlantic Ocean along the Atlantic meridional transect (AMT) 12 cruise from the Falkland Islands to the U.K.

## MATERIALS AND METHODS

**Reagents.** All reagents were of analytical grade or better and were purchased from Sigma-Aldrich (Dorset, U.K.) unless otherwise stated. Ultrapure Milli-Q water (resistivity  $\geq 18 \text{ M}\Omega \text{ cm}$ ) was used throughout. Due to solubility considerations, the Fe(III) salt used was iron(III) nitrilotriacetate (Fe(NTA)). A 1 mM stock Fe(NTA) solution was prepared by mixing  $\text{FeCl}_3$  and nitrilotriacetic acid (NTA) in water. Iron(III) standards were prepared by dilution from the stock solution.

Seawater samples were collected from the North Atlantic Ocean during the AMT cruise (12 May–17 June 2003) running from the Falkland Islands to the U.K. (<http://www.pml.ac.uk/amt>). To prevent contamination, the seawater samples were unfiltered and collected at varying depths from 3 to 303 m at an exact position of  $49^\circ 39.0' \text{N}$ ,  $18^\circ 31.8' \text{W}$ . The samples were kept in a freezer ( $-20^\circ \text{C}$ ) and were thawed before use. Since the pH of the seawater samples was  $\sim 8.0$ , no pH adjustment of the samples was made prior to use. The certified seawater reference material, NASS-5, was obtained from the National Research Council of Canada (Marine Analytical Chemistry Standards Program). As the NASS-5 seawater is acidic and has a high iron concentration, the standard was buffered by dilution in tricine buffer (pH 8) prior to analysis.

**Bacterial Growth, Extraction, and Purification of Parabactin.** Parabactin (Figure 1), excreted by the bacterium *P. denitrificans* wild type (PD 1222),<sup>25</sup> was extracted from the culture supernatant using the following protocol. Bacterial samples of *P. denitrificans* were initially grown aerobically in a defined minimal ammonium medium. This medium contained the following (per L): succinic acid, 5.9 g; NaOH, 4.0 g;  $\text{KH}_2\text{PO}_4$ , 4.0 g;  $\text{Na}_2\text{HPO}_4$ , 4.9 g;  $\text{Mg}_2\text{SO}_4 \cdot 7\text{H}_2\text{O}$ , 0.2 g;  $\text{Na}_2\text{MoO}_4 \cdot 2\text{H}_2\text{O}$ , 0.15 g;  $\text{NH}_4\text{Cl}$ , 1.6 g. After autoclaving the defined minimal medium,  $\text{MnSO}_4$ , which had been sterilized by filtration, was added to the medium at a concentration of  $4.5 \mu\text{M}$ .

Bacterial samples of *P. denitrificans* from frozen glycerol stock were initially grown in 100 mL of defined minimal ammonium medium under aerobic conditions at  $30^\circ \text{C}$  for 24 h. Aliquots (6 mL) of the resulting bacterial stock were subsequently inoculated into six flasks (2 L), each containing 750 mL of sterile minimal ammonium medium. The flasks were sealed and aerobic growth was induced by shaking (200 rpm) at  $30^\circ \text{C}$  for 48 h. The culture broth was centrifuged (Beckmann Avanti J-20 centrifuge) at 7000 rpm for 30 min at  $4^\circ \text{C}$  resulting in cell compaction. The resultant yellow supernatant ( $\sim 4 \text{ L}$  in total) containing parabactin was decanted from the brown bacterial pellet and stored at  $4^\circ \text{C}$  for further purification.

The extraction of parabactin from the culture supernatant (4 L) of *P. denitrificans* was achieved based on a method described by Tait.<sup>15</sup> First the culture supernatant was acidified to pH 2 with concentrated HCl (12 M) in order to ensure that the parabactin was in the free, uncomplexed form. Next, the acidified culture supernatant (700 mL) was extracted four times with ethyl acetate

(150 mL). The bottom aqueous layer was discarded, and the top ethyl acetate layer containing parabactin was kept for a second extraction with 10% (w/v) sodium hydrogen carbonate. Two layers were again obtained, and the top ethyl acetate layer was kept for further purification. The pooled ethyl acetate layer was dried over sodium sulfate and the solvent evaporated leaving a yellow residue at the bottom of the round-bottom flask. The solid was dissolved in 10 mL of toluene/ethyl acetate (4:1 v/v) resulting in a yellow solution. Silicic acid column chromatography was used to remove further unwanted products while the parabactin was eluted from the column using a toluene/ethyl acetate (1:1 v/v) solvent mix. After evaporation of the solvent mix, the resulting white residue was dissolved in 0.5 mL of ethanol, which gave a white suspension when added, with stirring, to 15 mL of water. The suspension was centrifuged and the water subsequently decanted. The remaining white pellet was redissolved in a minimum of ethanol, and dried in vacuo to give a white powder (parabactin). For a 6-L growth of *P. denitrificans*,  $\sim 40 \text{ mg}$  of parabactin was obtained.

Characterization of the parabactin product (white powder) was achieved using  $^1\text{H}$  NMR (400 MHz), low-resolution electron ionization (EI) and fast atom bombardment mass spectrometry (FAB-MS). Parabactin,  $\text{C}_{32}\text{H}_{36}\text{N}_4\text{O}_9$ , has a theoretical molecular weight of 620.67. In the EI-MS, a molecular ion  $\text{M}^+$  peak at 620.2 was obtained corresponding to the true molecular weight of parabactin.<sup>26</sup> Two peaks at 621.3 and 643.3, which were attributed to  $(\text{M} + \text{H})^+$  and  $(\text{M} + \text{Na})^+$  ions, respectively,<sup>27</sup> were seen in the FAB-MS. The  $^1\text{H}$  NMR spectrum of the purified parabactin was similar to that reported by Bergeron<sup>28</sup> with the  $\beta$ ,  $\alpha$ , and  $\gamma$  oxazoline protons at approximately 5.40, 4.60, and 1.45 ppm, respectively. The most outstanding feature of the NMR spectrum of parabactin was linked to the duplicity of the NMR signals. This was especially apparent when looking at the set of doublets associated with  $\alpha$  and  $\gamma$  oxazoline protons. In addition, the protons corresponding to the catechol hydroxyls were observed around 11.77 ppm while aromatic protons were enclosed in an envelope ranging from 6.40 to 7.80 ppm. These spectroscopic features are all characteristic of a pure sample of parabactin.

**Instrumentation.** Fluorescence spectra were measured using a Fluoromax 2 fluorometer (ISA Instruments S.A., Inc.) used in combination with a quartz flow cell (Starna Optiglass Ltd.). A five-way injection valve (Omnifit) connected to a peristaltic pump (Pharmacia Biotech) was used for flow cell measurements. All capillary tubings were PTFE tubing with an outside diameter of 1.8 mm and internal diameter of 1.1 mm (Amersham Biosciences). UV–visible absorbance spectra were recorded on a Hitachi U-3010 spectrophotometer, and pH was measured with an Accumet Basic pH meter (Fisher Scientific). Parabactin was dissolved in different solvents including ethanol, aqueous solution pH 3.1 and 8.0, and 0.01 M Tricine buffer, pH 8. The absorption and fluorescence spectra of parabactin in these different solutions were recorded.

**Ion Interference Studies.** Stock solutions of various salts were prepared to study potential interferences for the determination of Fe(III) using the parabactin. The following ions were studied:  $\text{Na}^+$ ,  $\text{K}^+$ ,  $\text{Ca}^{2+}$ ,  $\text{Mg}^{2+}$ ,  $\text{Cu}^{2+}$ ,  $\text{Ni}^{2+}$ ,  $\text{Zn}^{2+}$ ,  $\text{Pd}^{2+}$ ,  $\text{Al}^{3+}$ ,  $\text{Mn}^{2+}$ ,

(25) De Vries, G. E.; Harms, N.; Hoogendijk, J.; Stouthamer, A. H. *Arch. Microbiol.* **1989**, *152*, 52–57.

(26) Buckley, G. M.; Pattenden, G.; Whiting, D. A. *Tetrahedron* **1994**, *50*, 11781–11792.

(27) Miyasaka, T.; Nagao, Y.; Fujita, E.; Sakurai, H.; Ishizu, K. *J. Chem. Soc., Perkin Trans. 2* **1987**, 1543–1549.

(28) Bergeron, R. J. *Chem. Rev.* **1984**, *84*, 587–602.



$\text{Cr}^{3+}$ ,  $\text{Fe}^{2+}$ ,  $\text{Co}^{2+}$ ,  $\text{Sr}^{2+}$ ,  $\text{F}^-$ ,  $\text{Cl}^-$ ,  $\text{CO}_3^{2-}$ ,  $\text{SO}_4^{2-}$ , and  $\text{NO}_3^-$ . Different ratios of these "interference" ions to  $\text{Fe(III)}$  concentrations (1:1–1000:1) were introduced into a 5.0  $\mu\text{M}$  parabactin + 5.0 nM  $\text{Fe(NTA)}$  solution in 0.01 M tricine buffer, pH 8.0. The degree of interference was evaluated by fluorescence measurements.

#### Encapsulation of Parabactin in a Silica Sol–Gel Matrix.

The optimized synthetic procedure for the encapsulation of the parabactin in a silica sol–gel matrix for the measurement of  $\text{Fe(III)}$  is reported. The formation of the sol–gel films was based on the method of Aylott et al.<sup>29</sup> A silica sol–gel comprising tetramethyl orthosilicate (1.5 mL), deionized water (1 mL), methanol (1.5 mL), and  $\text{HCl}$  (0.05M, 0.1 mL) was sonicated on ice for 30 min and stored at  $-20^\circ\text{C}$  for 36–72 h to allow complete hydrolysis to occur. The sonicated sol (90  $\mu\text{L}$ ) was then added to 10  $\mu\text{L}$  of a methanolic solution of 20 mM parabactin. To prevent gelation, the parabactin doped sol–gel mixture was stored on ice prior to film manufacture. The films were cast within 30 min of making the parabactin sol–gel solution. Quartz substrates ( $45 \times 13 \times 1$  mm) from Apex Services (Cambridge, UK) were wiped clean with methanol. The quartz substrate was mounted on the rotating base of a spin-coating instrument (Headway Research Ltd., Garland, TX) and held in place by an applied vacuum. Methanol (2 mL) was pipetted onto the substrate surface, while it was spinning at 1750 rpm, to ensure a clean surface. The spin-coating instrument was stopped, and the parabactin-doped sol–gel solution (100  $\mu\text{L}$ ) was pipetted onto the substrate, which was then spun at 1750 rpm for 30 s. The coated quartz substrate was placed in a covered Petri dish and allowed to dry overnight at ambient temperature ( $20^\circ\text{C}$ ). The following day, the prepared substrate was immersed in 0.01 M tricine buffer, pH 8.0, and allowed to equilibrate for 24 h prior to  $\text{Fe(III)}$  sensing measurements. This method produced optically transparent, crack-free sol–gel films, with an initial thickness<sup>29</sup> of  $\sim 5 \mu\text{m}$ .

**Procedure for  $\text{Fe(III)}$  Determination.** The sensor system was based on flow cell technology consisting of two quartz panels. The sol–gel-coated quartz substrate was used as the front panel, while the back panel, with inlet and outlet, contained a 0.3-mL volume etched into the quartz surface to allow the flow of various solutions across the sol–gel-encapsulated parabactin. The flow cell was housed in the sample compartment of the fluorescence spectrometer. A five-way rotary valve, connected to a peristaltic pump, was used to pass the appropriate solution over the sol–gel film. Buffer (0.01 M tricine, pH 8.0),  $\text{Fe(III)}$  standard solution of varying concentrations (0.05–10.20 nM), and seawater samples or the regeneration solution (0.10 M  $\text{HCl}$ ) were pumped alternatively through the flow cell.

The sensing of  $\text{Fe(III)}$  was achieved as follows: Tricine buffer was passed over the sensor surface for 3 min. Next the sample, either seawater or  $\text{Fe(NTA)}$  standard solution, was passed over the sensor to allow  $\text{Fe(III)}$  determination. The fluorescence intensity at 460 nm (excitation at 311 nm) was recorded for a period of 10 min. The formation of the  $\text{Fe}$ –parabactin complex was evidenced by the decrease in the fluorescence intensity at 460 nm when the  $\text{Fe(III)}$  solution was passed through the flow cell. Following the 10-min measurement period, 0.10 M  $\text{HCl}$  was pumped over the sensor surface for 3 min to dissociate the iron–

parabactin complex. Subsequently, 0.01 M tricine buffer was passed through the flow cell to restore the fluorescence intensity to the initial level, prior to a further measurement. The full measurement–regeneration cycle took  $\sim 20$  min, and each measurement of seawater sample/standard was performed in duplicate.

The concentration of  $\text{Fe(III)}$  in seawater samples was determined by a standard calibration curve and by the standard additions method. For the latter calibration method, 5 mL of a seawater sample was spiked with known concentrations of  $\text{Fe(NTA)}$  (50, 100, 150, 200 pM) and the seawater samples were analyzed using the flow cell procedure described above. A standard additions curve of decrease in fluorescence intensity (after 10 min) versus concentration of  $\text{Fe(NTA)}$  added was plotted, and the concentration of iron(III) in the seawater sample was determined by extrapolation of the linear calibration curve.

## RESULTS AND DISCUSSION

**Absorption and Fluorescence Spectra of Parabactin.** The absorption spectrum of the purified parabactin, in ethanol, is shown in Figure 2a. In ethanol, parabactin exhibits three absorption bands centered at 210, 250, and 311 nm. These absorption band maxima are similar to those reported by Peterson and Neilands.<sup>30</sup> In aqueous solution at pH 3.1, parabactin has absorption bands at 210, 250, and 311 nm, whereas at an increased pH of 8.0, the absorption bands are red-shifted to 210, 253, and 316 nm (Figure 2a).

Peterson and Neilands<sup>30</sup> and Tait<sup>16</sup> have reported the absorption spectrum of parabactin in various solvents; however, to our knowledge, the fluorescence emission and excitation spectra of parabactin have not been published. The fluorescence emission and excitation spectra of parabactin in ethanol and aqueous solutions at pH 3.1 and 8.0 are shown in Figure 2 (b and c, respectively). Upon excitation at 311 nm, the maximum emission of parabactin in aqueous solution at pH 3.1, at pH 8.0, and in ethanol occurs at 460, 440, and 401 nm, respectively. The fluorescence excitation spectrum of parabactin in ethanol ( $\lambda_{\text{em}} = 401$  nm) has two maxima at 255 and 332 nm. The excitation spectrum of parabactin in aqueous solutions pH 3.1 and 8.0 has maxima at 262, 314 nm and 258, 334 nm, respectively. Thus, changes in pH influence the wavelength position of the fluorescence emission band of parabactin in aqueous solution resulting in a blue shift in the emission band when the pH is increased from 3.1 to 8.0. It should be noted that the excitation and emission spectra are noncorrected spectra of parabactin, which may account for the differences between the absorption and excitation spectra seen in Figure 2a and c.

Initially, the UV–visible and fluorescence characterization of the  $\text{Fe(III)}$  coordination with parabactin was determined in ethanol. Following assessment of numerous buffers, the spectroscopic characterization of the  $\text{Fe(III)}$  binding with parabactin in 0.01 M tricine buffer (pH 8) was achieved. The absorption spectrum of the free parabactin, at pH 8, exhibits absorption bands at 210, 250, and 311 nm. When  $\text{Fe(III)}$  was added to the parabactin, a wine-red complex was formed with an additional absorption band centered at 500 nm. The intensity of fluorescence is quenched when increasing concentrations of  $\text{Fe(III)}$  are added to a solution

(29) Aylott, J. W.; Richardson, D. J.; Russell, D. A. *Chem. Mater.* **1997**, *9*, 2261–2263.

(30) Peterson, T.; Neilands, J. B. *Tetrahedron Lett.* **1979**, *50*, 4805–4808.

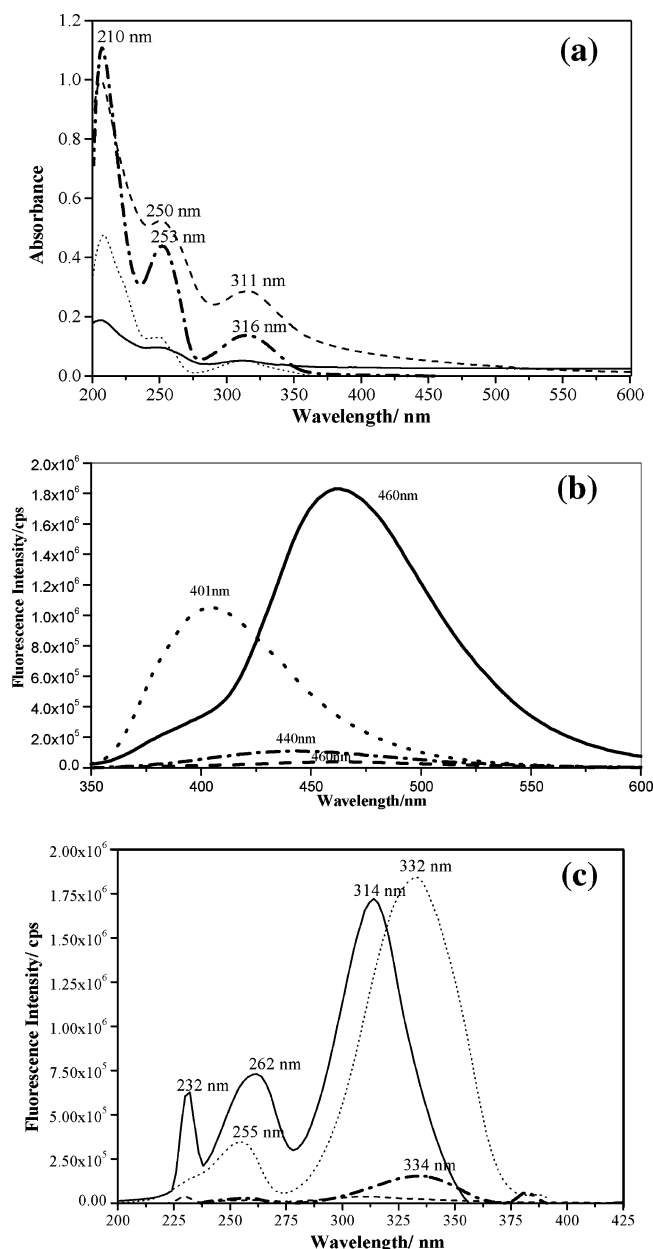


**Figure 2.** (a) Absorption spectrum of 5 μM parabactin in ethanol (dot); 23 μM parabactin in aqueous solution, pH 3.1 (dash); 15 μM parabactin in aqueous solution, pH 8.0 (dash dot); and sol-gel-encapsulated parabactin (solid). (b) Fluorescence emission spectra ( $\lambda_{\text{ex}} = 311 \text{ nm}$ ) of 2 μM parabactin in ethanol (dot); 1 μM parabactin in aqueous solution, pH 3.1 (dash) and pH 8.0 (dash dot); and sol-gel-encapsulated parabactin (solid). (c) Fluorescence excitation spectra of 2 μM parabactin in ethanol (dot); 1 μM parabactin in aqueous solution, pH 3.1 (dash) and pH 8.0 (dash dot); and sol-gel-encapsulated parabactin (solid) ( $\lambda_{\text{em}} = 460, 440, 401, \text{ and } 460 \text{ nm}$  respectively).

of parabactin. Importantly, the quenching of the fluorescence signal as a function of Fe(III) concentration can be quantified using the Stern–Volmer relationship to provide the basis for quantitative Fe(III) measurements in seawater.

#### Spectral Characteristics of the Encapsulated Parabactin.

The absorption and fluorescence spectra of the encapsulated parabactin were compared to that of parabactin in solution in order to determine whether entrapment of parabactin in a sol–gel matrix altered the observed optical properties. From Figure 2a, it can be

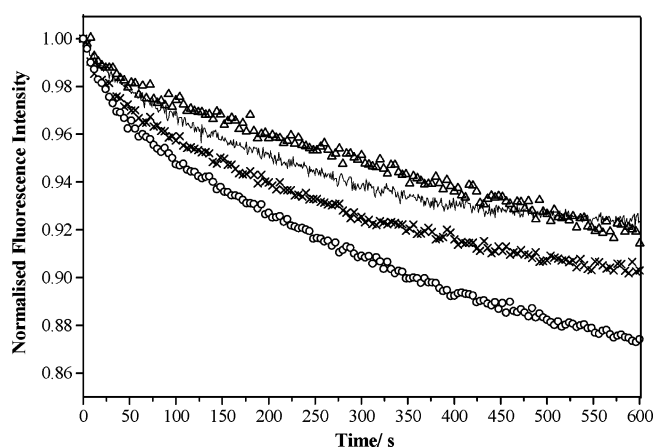


**Figure 3.** Response curve of encapsulated parabactin sensor flushed with Fe(III) solutions of 1.00 (circles), 0.50 (crosses), 0.10 (solid line), and 0.05 nM (triangles).

seen that the absorption spectrum of the encapsulated parabactin exhibited absorption bands at 210, 250, and 311 nm that were similar to parabactin in ethanol and aqueous solution at pH 3.1 but not at pH 8.0. Additionally, the intensity of fluorescence emission of the immobilized parabactin was maximal at 460 nm (Figure 2b), similar to that observed for the emission of the siderophore at pH 3.1. The wavelength of maximum fluorescence intensity of the encapsulated parabactin can be attributed to the environment in which the parabactin fluorophore was located within the sol–gel matrix. Previous studies have shown that, when sol–gels are manufactured via the acid catalyst procedure, the microenvironment of the pores (where the biomolecule is entrapped) is acidic.<sup>31</sup> Since the preparation of the sol in this work was acid catalyzed, when parabactin was immobilized in the sol–gel matrix, it would be found in an acidic environment. A similar inference can be drawn from the fluorescence excitation spectrum (Figure 2c) where two maxima at 262 and 314 nm are observed for the encapsulated parabactin, identical to those obtained for the parabactin in aqueous solution at pH 3.1.

**Characterization of the Parabactin Sensor.** Figure 3 illustrates the typical response curves of the encapsulated parabactin biosensor when subjected to iron(III) solutions of differing concentrations. When solutions of Fe(III) were pumped through the flow cell, a significant decrease in fluorescence intensity was achieved that was proportional to the concentration of Fe(III) in solution. The decrease in fluorescence intensity at 460 nm with each Fe(III) concentration was used to construct a calibration curve. The calibration curve, obtained by plotting decrease in fluorescence intensity, after 10 min, versus Fe(III) concentration, was linear ( $y = 0.049x + 0.074$ ) from 0.05 to 1.00 nM with a correlation coefficient of 0.987. The detection limit ( $3\delta$ ; with  $\delta$  defined as the standard deviation of the blank) was determined to be 40 pM while the relative standard deviation was 6% ( $n = 10$ ) for a 1.00 nM Fe(III) standard. The accuracy of the parabactin biosensor was determined by analyzing a standard reference seawater sample, NASS-5, obtained from the National Research Council of Canada. Although the NASS-5 standard has a relatively high iron concentration, typically 5-fold greater than the sub-nanomolar Fe(III) concentrations found in the Southern Ocean,

(31) Brennan, J. D. *Appl. Spectrosc.* **1999**, *53*, 106A–121A.

**Table 1. Comparison of the Dissolved Iron Values Determined by the Parabactin Biosensor and the Certified Values for NASS-5 Standard Seawater Sample<sup>a</sup>**

standard solution	iron concentration (nM)	
	certified value	parabactin biosensor
NASS-5	3.71 ± 0.63	3.24 ± 0.35

<sup>a</sup> Uncertainties represent 95% confidence interval.

for example,<sup>32</sup> it was used because it contains the lowest iron concentration of any commercially available standard reference material. The comparative results of the accepted value and that determined by the parabactin biosensor are shown in Table 1. It should be noted that the certified value for the NASS-5 standard is for the total dissolved iron present in the seawater. However, it is clear that there is good agreement between the two values for the NASS-5 standard and that accurate total iron concentration measurements can be achieved using our parabactin biosensor.

The interference of various cations and anions likely to be present within seawater on the fluorometric determination of Fe(III) was investigated. The tolerance limit was taken as the concentration of the interference ion that caused a  $\pm 5\%$  change in the fluorescence intensity, and the results are presented in the Supporting Information. Of the numerous ions tested,  $\text{Zn}^{2+}$ ,  $\text{Mn}^{2+}$ , and  $\text{Cr}^{3+}$  caused a significant interfering signal at concentrations of  $\geq 2.5$ , 0.5, and 5.0  $\mu\text{M}$ , respectively, when an Fe(III) concentration of 5.0 nM was measured. In the Southern Ocean, the concentration of zinc ions is  $\sim 2.0$  nM,<sup>33</sup> while in the NE Atlantic Ocean, total zinc concentrations range from 0.3 nM in surface waters to 2.0 nM at 2000-m depth.<sup>34</sup> In the eastern Atlantic Ocean, total dissolvable manganese concentrations are in the range of 0.9–2.1 nM in surface waters (upper 2000 m) and decrease to  $\sim 0.2$  nM in deeper waters (5000 m).<sup>35</sup> Chromium concentrations in the NW Pacific Ocean range from 0.1 to 1.4 nM.<sup>36</sup> Therefore, since  $\text{Zn}^{2+}$ ,  $\text{Mn}^{2+}$ , and  $\text{Cr}^{3+}$  concentrations in these Oceanic waters are maximally 2.0, 2.1, and 1.4 nM, respectively, these ions would not interfere with the determination of Fe(III), even at the lowest 50 pM level, using the parabactin biosensor.

**Seawater Samples.** The parabactin biosensor was applied to the analysis of Fe(III) concentrations in unfiltered seawater samples collected during a recent AMT12 cruise on board the *RRS James Clark Ross*. The site of sample collection was the North Atlantic Ocean (49°39.0'N, 18°31.8'W) at varying depths from 3 to 303 m. The vertical distribution of the measured Fe(III) at the collection site is shown in Figure 4. Iron concentrations increase from low values,  $<100$  pM, in the surface waters to 700–1000

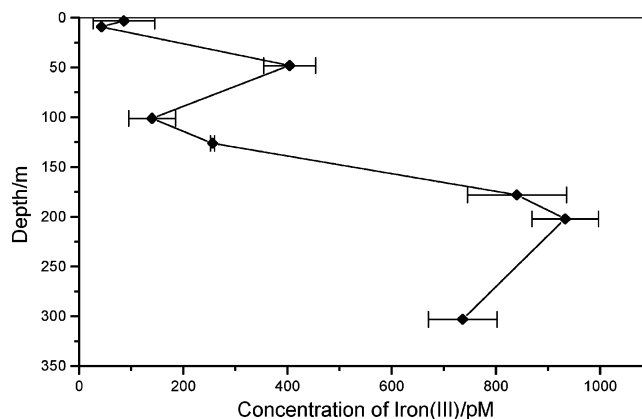


**Figure 4.** Bioavailable Fe(III) concentration profile versus depth for the North Atlantic Ocean samples. (Each point is the average of 2 measurements.)

pM at 300 m. The low values observed in the surface waters are a result of active biological uptake associated with photosynthesis, while the higher values below the illuminated waters are due to reduced uptake and active regeneration of iron from sinking biological sources. Similar iron profiles have been reported from this area of the North Atlantic Ocean,<sup>4,37–39</sup> further demonstrating the validity of the siderophore biosensor reported here.

## CONCLUSIONS

This work has successfully established that the siderophore parabactin, obtained from the bacterium *P. denitrificans*, can be encapsulated within a sol–gel matrix and developed into a reusable biosensor for the selective determination of Fe(III) concentrations in seawater samples. The method does not require a preconcentration step and can measure Fe(III) in the nanomolar and subnanomolar concentration range without any interference from cations and anions present in oceanic waters. The sol–gel-encapsulated parabactin could be readily coupled with miniaturized instrumentation to provide small “footprint” devices for shipboard deployment. The results show that the developed parabactin biosensor enables the direct measurement of the ultratrace bioavailable fraction of iron species found in oceanic waters, such as the Southern Ocean, and consequently provides the necessary tool for analytical environmental scientists to establish the factors regulating iron concentrations within the World’s oceans.

## ACKNOWLEDGMENT

Financial support was received from the EPSRC (Metrology for Life Sciences; Grant GR/N19663/01) with additional support for C.K.S.C.C.L. from the ORS awards scheme. Oceanic water samples were collected during the NERC funded AMT12 cruise; collection assistance from Dr. Peter Statham and Florence Nedelec (Southampton Oceanography Centre, U.K.) is gratefully acknowledged.

## SUPPORTING INFORMATION AVAILABLE

Additional information as noted in text. This material is available free of charge via the Internet at <http://pubs.acs.org>.

Received for review February 2, 2006. Accepted May 23, 2006.

AC060223T

- (32) Obata, H.; van den Berg, C. M. G. *Anal. Chem.* **2001**, *73*, 2522–2528.  
 (33) Frew, R.; Bowie, A.; Croot, P.; Pickmere, S. *Deep-Sea Res., Part II* **2001**, *48*, 2467–2481.  
 (34) Ellwood, M. J.; van de Berg, C. M. G. *Mar. Chem.* **2000**, *68*, 295–306.  
 (35) Statham, P. J.; Yeats, P. A.; Landing, W. M. *Mar. Chem.* **1998**, *61*, 55–68.  
 (36) Isshiki, K.; Nakayama, E. *Anal. Sci.* **2001**, *17*, 11571–11574.  
 (37) Bowie, A. R.; Whitworth, D. J.; Achterberg, E. P.; Mantoura, R. F. C.; Worsfold, P. J. *Deep-Sea Res., Part I* **2002**, *49*, 605–636.  
 (38) Measures, C. I.; Vink, S. *Deep-Sea Res., Part II* **2001**, *48*, 3913–3941.  
 (39) Bowie, A. R.; Achterberg, E. P.; Sedwick, P. N.; Ussher, S.; Worsfold, P. J. *Environ. Sci. Technol.* **2002**, *36*, 4600–4607.